Journal of Physics: Conference Series **1602** (2020) 012015 doi:10.1088/1742-6596/1602/1/012015

Direct photon production and scaling properties in large and small system collisions

Vladimir Khachatryan for the PHENIX Collaboration

Department of Physics and Astronomy, Stony Brook University, Stony Brook, New York 11794-3800, USA

E-mail: vladimir.khachatryan@stonybrook.edu

Abstract. We present recent measurement results of low momentum direct photons obtained by the PHENIX collaboration from Cu+Cu at 200 GeV and Au+Au at 200 GeV, 62.4 GeV, 39 GeV, as well as from p+p and p+Au at 200 GeV. In these measurements a large excess over the scaled reference p+p yield of direct photons is observed in A+A collisions, and a non-zero excess over the scaled p+p yield is found within systematic uncertainties in central p+Au collisions. Based upon the comparison between this recent data and the PHENIX published Au+Au data at 200 GeV, along with including the ALICE Pb+Pb data at 2760 GeV, PHENIX has found that the direct photon p_T-spectra and their integrated yield, dN_γ/dy, above 1 GeV/c in p_T follow a universal scaling as a function of the charged-hadron multiplicity, $(dN_{ch}/d\eta)^\alpha$, with $\alpha = 1.25$. Within experimental uncertainties, the direct photon scaling properties observed in large collision systems is independent of the colliding species, collision centrality selection and center-of-mass energy. One possible explanation is that the photon radiation sources may have similar properties for all colliding large systems across different energies. There is also another trend coming from integrated direct photon p_T-spectra of small systems, which suggests that the QGP turn off/on transition region may exist between large and small system collisions.

1. Introduction

Direct photons produced in (ultra)relativistic heavy ion collisions are considered to be a unique probe for studying the entire space-time evolution of colliding systems, with which one can extract important information on thermal properties and collective behavior of the hot fireball of Quark Gluon Plasma (QGP). These photons being color blind probes, contrary to partons, directly probe the conditions of their production environment at the time of production, and due to the small cross section with the collision-produced medium like QGP, they leave the collision region virtually unmodified with no final state interactions.

Direct photons describe the excess yield, which one can obtain by subtracting the hadronic decay photon yield (mostly from π^0 and η decays) from the total inclusive photon yield. In general, the direct photons have thermal and non-thermal origins. According to current understanding, the thermal photons originate from the pre-equilibrium phase, the QGP phase and the late hadronic gas (HG) phase. This type of photons dominate over the low transverse momentum region. The non-thermal photons, dominating over the high-p_T region, come from initial hard scattering processes (prompt photons) like quark anti-quark annihilation or QCD Compton scattering among the incoming and outgoing partons, and from the pre-equilibrium phase as well.

PHENIX has measured low momentum direct photon p_T-spectra in Au+Au collisions at $\sqrt{s_{NN}} = 200\,\text{GeV}$, with a large excess yield observed at $p_T < 3\,\text{GeV/c}$ above the hard scattering contribution given by a reference $p+p$ yield scaled by the number of binary collisions, N_{coll}, [1, 2]. PHENIX has also measured large anisotropies of direct photons in Au+Au collisions at $\sqrt{s_{NN}} = 200\,\text{GeV}$ with respect to the reaction plane [3]. After these large yield and large anisotropy measurements, a challenging problem arose, known as "direct (thermal) photon flow puzzle", where different theoretical models basically fall short in describing these two quantities simultaneously. The best models and mechanisms have mixed success in doing so [4, 5, 6, 7, 8, 9, 10, 11]. In order to help resolve this puzzle, and in particular to reconcile the assumed photon sources with the calculated invariant yields, PHENIX has continued to measure low momentum direct photons by varying the system size and geometry, going from large to small collision systems, along with changing the center-of-mass (beam) energy for large systems. In this proceedings we report on these results and other related findings by PHENIX.

2. Direct photon measurement techniques and their p_T-spectra from large systems

So far PHENIX has analyzed wealth of its data sets available for direct photon analysis by exploiting three different analysis methods – the internal conversion method [1], the external conversion method [2] and the calorimeter method [12].

- In the internal conversion method one uses virtual photons that internally convert to low mass dilepton pairs ($\gamma^* \to e^+e^-$).
- In the external conversion method one uses real photons that externally convert to dilepton pairs ($\gamma \to e^+e^-$) in a well selected detector material.
- In the calorimeter method the photons are reconstructed directly from their energy deposition in electromagnetic calorimeters.

Direct photon p_T-spectra in Au+Au collisions at 200 GeV in Ref. [1] have been obtained with the internal conversion method, which recently has also been used to obtain the spectra in Cu+Cu at 200 GeV [13] (see the left panel of Fig. 1). The PHENIX measurements with 2010 Au+Au datasets were accomplished via the external conversion method, where the photons were measured through their conversions to e^+e^- pairs in the readout plane and electronics of the PHENIX detector subsystem called Hadron Blind Detector, or in short, HBD backplane. Here one used conversions happening at fixed radius equal to 60 cm from the event vertex. The HBD backplane had $X/X_0 \sim 3\%$ radiation length. So the direct photon invariant yield results in Au+Au collisions at 200 GeV from Ref. [2] have been obtained by the external conversion method with the HBD backplane, which has also been used to analyze 2010 Au+Au datasets for obtaining the yield at lower beam energies – 62.4 GeV and 39 GeV [14, 15, 16].

STAR collaboration has reported direct photon measurements in Au+Au at 200 GeV [17], with invariant yields significantly lower than those from the available PHENIX results. In order to address this observed discrepancy between the two experiments, an independent measurement was accomplished by PHENIX, utilizing the Au+Au dataset with high statistics taken in 2014 [18]. The external conversion method has been used again, however, in that analysis the photons were measured through their conversions to e^+e^- pairs at the Silicon Vertex Tracker (VTX), which had the radiation length of $X/X_0 \sim 14\%$.

In order to construct the direct photon p_T-spectra in the external conversion method, first by using the *Double Ratio Tagging Method* we should measure the direct photon relative yield, R_γ, which is an excess photon ratio defined as the ratio of the yield of true inclusive photons, γ^{incl}, to the yield of true photons coming from hadronic decays, γ^{hadron}. By dividing γ^{incl} and

γ^{hadron} by the yield of true photons from π^0 decays, we eventually get the following expression:

$$R_\gamma = \frac{\gamma^{incl}}{\gamma^{hadron}} = \frac{\frac{\gamma^{incl}}{\gamma^{\pi^0}}}{\frac{\gamma^{hadron}}{\gamma^{\pi^0}}} = \frac{\langle \epsilon f \rangle \left(\frac{N_\gamma^{incl}}{N_\gamma^{\pi^0}} \right)}{\frac{\gamma^{hadron}}{\gamma^{\pi^0}}}, \tag{1}$$

where the factor $\langle \epsilon f \rangle$ in the numerator in the right hand side is the efficiency and acceptance correction for pion tagging, which is obtained by running a full GEANT3-based simulation to account for the detector efficiency and acceptance effects. This factor quantifies the efficiency with which one can successfully tag a conversion pair as coming from a π^0 decay given that conversion pair is already reconstructed. And for measuring the π^0 yield, we pair the inclusive photons reconstructed from conversions with other photons reconstructed in the PHENIX electromagnetic calorimeter. N_γ^{incl} is the experimentally measured inclusive photon yield, and $N_\gamma^{\pi^0}$ is the measured tagged photo yield. Therefore the ratio $\frac{N_\gamma^{incl}}{N_\gamma^{\pi^0}}$ comes from data analysis. The second ratio in the denominator $\frac{\gamma^{hadron}}{\gamma^{\pi^0}}$, called Cocktail Ratio, is generated in a Monte Carlo simulation for estimating the ratio of hadronic decay photons to those of π^0 decays. The advantage of this method of double ratio tagging reduces the systematic uncertainty in R_γ measurements because the systematic uncertainties from the acceptance/efficiency corrections and conversion probability cancel out explicitly in the double ratio of Eq. (1).

After R_γ is measured, one can obtain the invariant yield using the following formula:

$$\text{Invariant Yield} = (R_\gamma - 1)\, \gamma^{hadron}. \tag{2}$$

The middle and right plots of Fig. 1 show the invariant yield of low momentum direct photons in minimum bias Au+Au at 62.4 GeV and 39 GeV. Fig. 2 shows the invariant yields of low momentum direct photons in Au+Au 0-20% and 20-40% centrality bins at 200 GeV obtained with the external conversion method with VTX. Fig. 3 shows similar yields but in 40-60% and 60-93% centrality bins. In Fig. 2 and Fig. 3 we see how four direct photon measurement results,

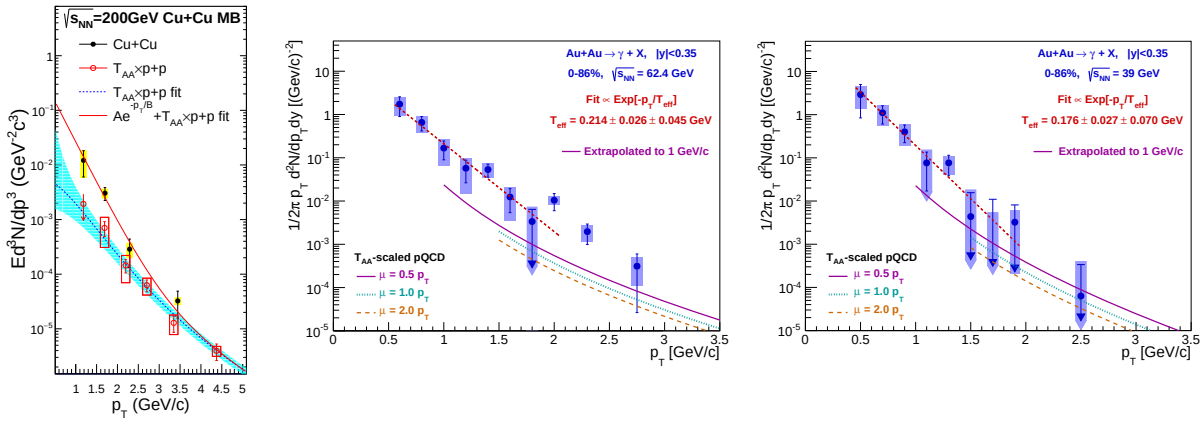

Figure 1. Direct photon p_T-spectra in Cu+Cu collisions at $\sqrt{s_{NN}} = 200$ GeV (left), measured by the internal conversion method [13]; in Au+Au collisions at $\sqrt{s_{NN}} = 62.4$ GeV (middle) and at $\sqrt{s_{NN}} = 39$ GeV (right), both measured by the external conversion method with HBD [14, 15, 16]. All the data are in minimum bias selection. The left plot also shows the N_{coll} scaled p+p fit, the middle and right plots show the N_{coll} scaled curves from pQCD calculations [19].

obtained independently of the analysis methods, are consistent with each other, which can be considered as validation of the PHENIX measurements.

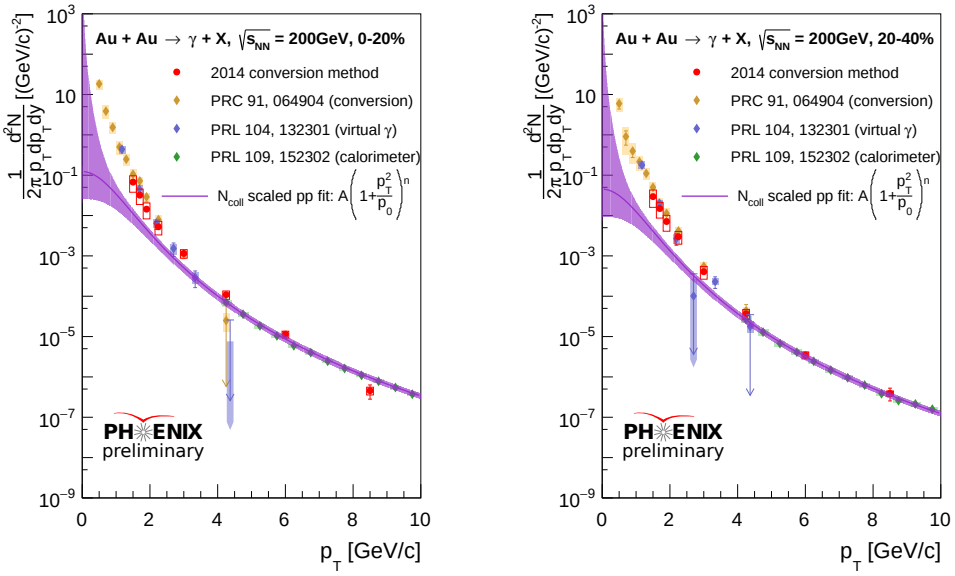

Figure 2. Direct photon p_T-spectra in Au+Au collisions in 0-20% (left) and 20-40% (right) centrality bins at $\sqrt{s_{NN}} = 200\,\text{GeV}$, measured by the external conversion method with VTX. A significant excess over the N_{coll} scaled p+p yield is observed below $p_T \sim 3\,\text{GeV/c}$ in these (semi-)central Au+Au collisions. The data are also consistent with the N_{coll} scaled p+p fit at high-p_T. This figure is from [18].

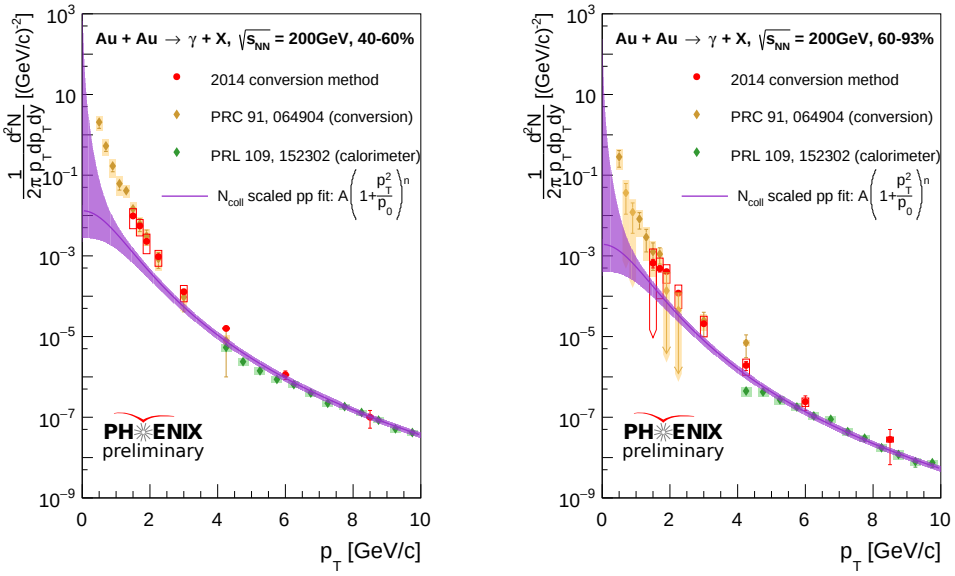

Figure 3. Direct photon p_T-spectra in Au+Au collisions in 40-60% (left) and 60-93% (right) centrality bins at $\sqrt{s_{NN}} = 200\,\text{GeV}$, measured by the external conversion method with VTX. The enhancement observed in Fig. 2 persists below $p_T \sim 3\,\text{GeV/c}$ in these (semi-)peripheral Au+Au collisions as well. This figure is from [18].

3. Direct photon p_T-spectra from small systems

PHENIX has also measured direct photon invariant cross sections in small system collisions, such as in p+p and minimum bias d+Au at 200 GeV [20]. These measurements have been accomplished by the internal conversion method. Nevertheless, there are recent measurements by the external conversion method with VTX, using p+p and p+Au data sets taken in 2015. These results are shown in Fig. 4. The left plot shows that consistent results are obtained in p+p collisions independent of the analysis method. The right plot shows a non-zero excess yield of low momentum direct photons within systematic uncertainties ($\sim 1\ \sigma$) in 0-5% p+Au collisions above the scaled p+p fit. This observation is consistent with a possible formation of QGP droplets in small systems [22]. See the caption of Fig. 4 for more details.

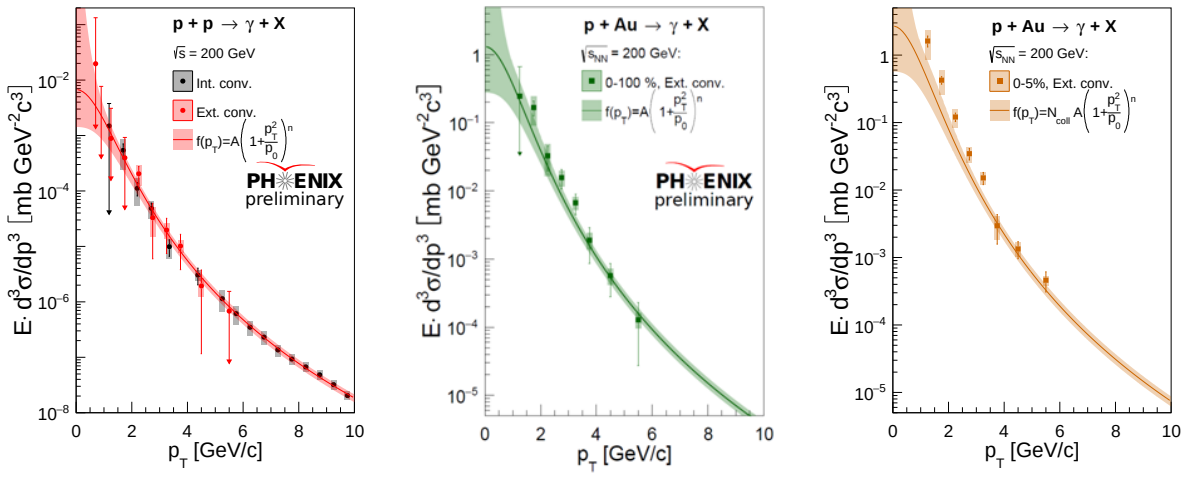

Figure 4. Invariant cross section in p+p and p+Au [15, 21]. The left plot shows the comparison of invariant cross sections measured in p+p collisions at $\sqrt{s_{NN}} = 200$ GeV from the internal conversions (black data points below 5 GeV/c), calorimeter method (black data points above 5 GeV/c), and external conversions (red data points). The shown fit is the most recent PHENIX fit obtained with all these p+p data points. The middle plot shows the invariant cross section from the external conversions with VTX in minimum bias p+Au collisions at $\sqrt{s_{NN}} = 200$ GeV; the right plot correspondingly shows the cross section in 0-5% p+Au at $\sqrt{s_{NN}} = 200$ GeV. The fit used in these plots are also used in the left panel of Fig. 1 as well as in Figs. 2 and 3.

4. Scaling properties of direct photons

Now we can discuss the scaling properties of direct photons, after having shown the p_T-spectra from large and small system collisions in the previous sections.

If we use the number of nucleons participating in A+A collisions, N_{part}, or the number of binary nucleon-nucleon interactions, N_{coll}, in this case one can compare direct photon data from different centrality classes (or system sizes) for a given center-of-mass energy. Meanwhile, when we compare data at different energies, we can first be based upon measuring the system size through the pseudorapidity density of produced charge particles at midrapidity, $dN_{ch}/d\eta|_{\eta\approx 0}$. This charged-hadron multiplicity can be used in such a case because it has an advantage of being an experimental observable. Moreover, it measures not only the volume but also the energy density. Besides, $dN_{ch}/d\eta|_{\eta\approx 0}$ itself has an interesting scaling relation with N_{coll}, as shown in Fig. 5. By this relation we can better understand the interplay between the system size and hard scattering processes. In Fig. 5 four datasets are simultaneously fitted by a power-law, with vertical and horizontal uncertainties of N_{coll} and $dN_{ch}/d\eta|_{\eta\approx 0}$, respectively [23, 24].

We see that N_{coll} scales like $(dN_{ch}/d\eta|_{\eta\approx 0})^{\alpha}$ with a $\sqrt{s_{NN}}$ -dependent proportionality factor called specific yield, SY. It is a logarithmically slowly increasing function with $\sqrt{s_{NN}}$ shown in the figure inset, and has the following form: SY $\approx 0.98 \log\left(\sqrt{s_{NN}}\right) - 1.83$. For the power α we find 1.25 ± 0.02. Thereby, one can use $(dN_{ch}/d\eta|_{\eta\approx 0})^{\alpha}$ in order to scale direct photon data for

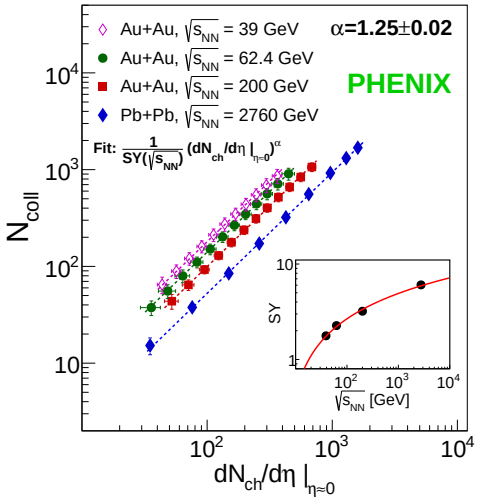

Figure 5. The scaling relation of N_{coll} vs. $dN_{ch}/d\eta|_{\eta=0}$ for four data sets in Au+Au at $\sqrt{s_{NN}} = 200\,\text{GeV}$, 62.4 GeV, 39 GeV and in Pb+Pb at $\sqrt{s_{NN}} = 2760\,\text{GeV}$. Across different beam energies N_{coll} is approximately proportional to $(dN_{ch}/d\eta|_{\eta\approx 0})^{1.25}$ with an energy-dependent proportionality factor shown in the inset. This figure is from [14].

different colliding species, centrality bins and beam energies.

Let us take, e.g., the direct photon p_T-spectra in minimum bias Au+Au collisions at 62.4 GeV and 39 GeV with the corresponding pQCD curves from Fig. 1, and normalize them by $(dN_{ch}/d\eta|_{\eta\approx 0})^{\alpha}$. It results in normalized data falling on top of each other at low-p_T, as shown in the panel (a) of Fig. 6. We also see that the normalized ISR p+p data coincide with the pQCD calculations at high-p_T within the quoted uncertainties. If we now take the direct photon data in Au+Au at 200 GeV from [1, 2, 12], and normalize them in the same way (panel (b)), then one can see that the normalized data are on top of each other at low- and high-p_T. At low-p_T they are clearly above the normalized p+p data, p+p fit and pQCD curve at 200 GeV. Finally, in the panel (c) we show the normalized data compared for different beam energies from 62.4 GeV to 2760 GeV. Again the conclusion is that all the data coincide at low-p_T within experimental uncertainties, while the expected difference with $\sqrt{s_{NN}}$ and N_{coll} scaling at high-p_T is seen too.

In Fig. 6 all the normalized data, p+p fit, pQCD curves are from [14, 15, 16, 21]. And they are obtained with Au+Au data from [1, 2, 12], Pb+Pb data from [25], p+p data at 200 GeV from [20], p+p data at 62.4/63 GeV from [26]/[27]. The empirical fit to the p+p data at 200 GeV is from [13, 14, 15, 21], the pQCD calculations at different beam energies are from [6, 19], and the data on $dN_{ch}/d\eta$ is from [23, 24]. Each error bar is the quadratic sum of the corresponding systematic and statistical uncertainties, and uncertainties on $dN_{ch}/d\eta$ are not included.

Another way to bring out more clearly some of the features of the discussed scaled data is to integrate the direct photon p_T-spectra above some p_T threshold value. The result, which is another representation of direct photon scaling is shown in Fig. 7 and Fig. 8, where the integrated yield dN_{γ}/dy grows faster than the multiplicity $dN_{ch}/d\eta|_{\eta\approx 0}$. The figures also show the integrated yield of the fit to p+p data, and of the three different pQCD calculations scaled by N_{coll} (which are extrapolated down to $p_T = 1\,\text{GeV/c}$). One of the interesting features is that the prompt photons (the purple band) and integrated pQCD lines have nearly the same slopes as the slope describing the large systems. The integrated A+A yield is a factor of ~ 10 larger than the expected yield from p+p.

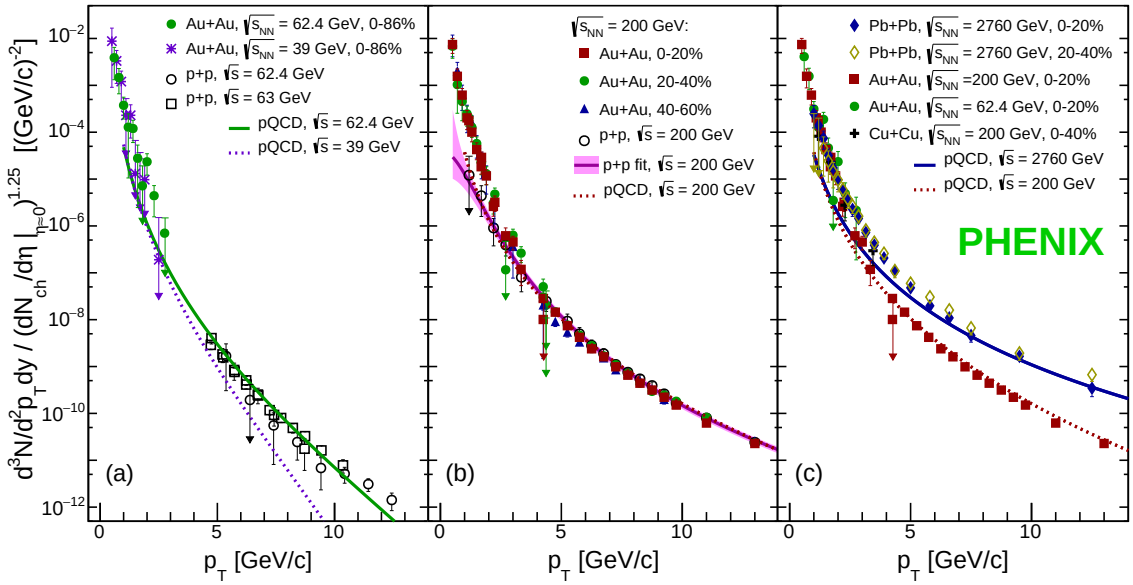

Figure 6. Direct photon p_T-spectra normalized by $(dN_{ch}/d\eta)^{\alpha}$ from [14, 15, 16]. The comparison is shown for minimum bias Au+Au collisions at 62.4 GeV and 39 GeV in the panel (a); for Au+Au data in three centrality bins at 200 GeV in the panel (b); and for different A+A systems at three beam energies in the panel (c). The panels (a) and (b) also show p+p data, and all the panels show pQCD calculations at respective energies.

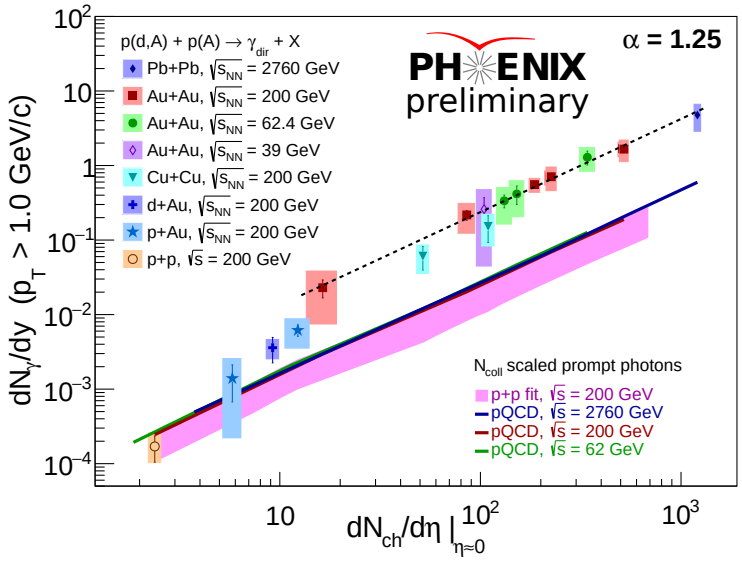

Figure 7. The integrated direct photon yield at $p_T > 1\,\mathrm{GeV/c}$ from various colliding systems as a function of the charged-hadron multiplicity at mid-rapidity. For integration some of the data are taken from Fig. 6. The other data are Cu+Cu from [13], p+Au data from Fig. 4 [15, 21], and d+Au data from [20]. The magenta band represents the N_{coll} scaled p+p data at $\sqrt{s_{NN}} = 200\,\mathrm{GeV}$, and the colored lines represent the N_{coll} scaled pQCD calculations at different energies. This figure is from [15, 16, 21].

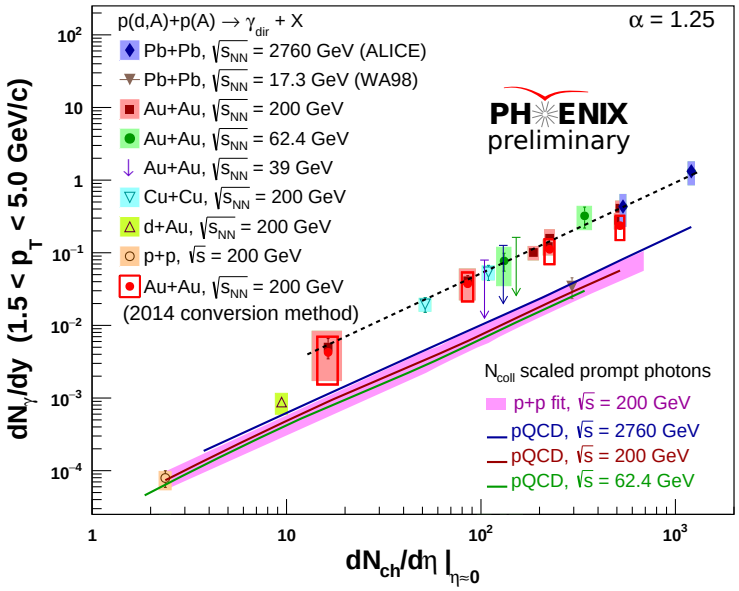

Figure 8. The integrated direct photon yield at $p_T > 1.5\,\mathrm{GeV/c}$ from various colliding systems as a function of the charged-hadron multiplicity at mid-rapidity. Most of the data are already shown in Fig. 7 but integrated above 1 GeV/c. One of the additions here is the p_T-integrated Au+Au data in four centrality bins at $\sqrt{s_{NN}} = 200\,\mathrm{GeV}$, the p_T-spectra of which are shown in Figs. 2 and 3. This figure is from [18].

Another quite interesting feature, which can be seen in Fig. 7 and Fig. 8, is that the PHENIX data from p+A and d+Au indicate a rapid onset of direct photon excess around $dN_{ch}/d\eta|_{\eta\approx0}$ in the region of $\sim 5 \div 20$. There seems to be another trend stemming from small systems different from that of large systems. Both trends suggest the existence of a QGP turn off or turn on transition region between both types of collision systems.

5. Summary and outlook

The PHENIX collaboration has measured low momentum direct photons in large system collisions, such as Au+Au at 200 GeV, 62.4 GeV, 39 GeV and in Cu+Cu at 200 GeV. Also in small system collisions, such as p+p, p+Au and d+Au at 200 GeV. Recent measurements in Au+Au at 200 GeV with higher statistical precision is consistent with the previous measurements in Au+Au at 200 GeV within experimental uncertainties. Having all the available data, including the data from the ALICE experiment, PHENIX has observed a surprising scaling behavior of low momentum direct photons in large systems: namely, the low- and high-p_T direct photon invariant yields in A+A collisions scale with N_{coll} at a given center-of-mass energy; meanwhile, across different energies N_{coll} is proportional to $(dN_{ch}/d\eta|_{\eta\approx0})^{\alpha}$; and for all energies the low-p_T yields scale like $(dN_{ch}/d\eta|_{\eta\approx0})^{\alpha}$. PHENIX has also discovered a non-zero excess of low momentum direct photons (within systematic uncertainties) at low-p_T in the most central p+Au collisions above N_{coll} scaled p+p fit, which is consistent with a formation of QGP droplets in small systems. The data in this low and narrow multiplicity region suggests the existence of a thermal transition region when we go from p+p to A+A systems or vice versa. More direct photon data should be analyzed before we have better understanding on what happens in this region. Besides, having more data from various colliding species and collision centrality selections at different beam energies may help constrain the sources of low momentum direct photons.

References

[1] Adare A *et al.* (PHENIX Collaboration) 2010 *Phys. Rev. Lett.* **104** 132301 (*Preprint* 0804.4168)
[2] Adare A *et al.* (PHENIX Collaboration) 2015 *Phys. Rev.* C **91** 064904 (*Preprint* 1405.3940)
[3] Adare A *et al.* (PHENIX Collaboration) 2016 *Phys. Rev.* C **94** 064901 (*Preprint* 1509.07758)
[4] van Hees H, He M and Rapp R 2015 *Nucl. Phys.* A **933** 256 (*Preprint* 1404.2846)
[5] Rapp R, van Hees H and He M 2014 *Nucl. Phys.* A **931** 696 (*Preprint*1408.0612)
[6] Paquet J-F *et al.* 2016 *Phys. Rev.* C **93** no. 4 044906 (*Preprint* 1509.06738)
[7] Shen C, Heinz U, Paquet J-F and Gale C 2014 *Phys. Rev.* C **89** 044910 (*Preprint* 1308.2440)
[8] Linnyk O, Cassing W and Bratkovskaya E 2014 *Phys. Rev. C* **89** 034908 (*Preprint* 1311.0279)
[9] Linnyk O, Konchakovski V, Steinert T, Cassing W and Bratkovskaya E 2015 *Phys. Rev.* C **92** 054914 (*Preprint* 1504.05699)
[10] Kim Y M, Lee C-H, Teaney D and Zahed I 2017 *Phys. Rev.* C **96** no. 1 015201 (*Preprint* 1610.06213)
[11] Lee C-H and Zahed I 2014 *Phys. Rev.* C **90** 025204 (*Preprint* 1403.1632)
[12] Afanasiev S *et al.* (PHENIX Collaboration) 2012 *Phys. Rev. Lett.* **109** 152302 (*Preprint* 1205.5759)
[13] Adare A *et al.* (PHENIX Collaboration) 2018 *Phys. Rev.* C **98** no. 5 054902 (*Preprint* 1805.04066)
[14] Adare A *et al.* (PHENIX Collaboration) 2019 *Phys. Rev. Lett.* **123** 022301 (*Preprint* 1805.04084)
[15] Khachatryan V (PHENIX Collaboration) 2019 *Nucl. Phys.* A **982** 763 (*Preprint* 1812.01841)
[16] Drees A (PHENIX Collaboration) 2019 *PoS* **HardProbes2018** 176
[17] Adamczyk L *et al.* (STAR Collaboration) 2017 *Phys. Lett.* B **770** 451 (*Preprint* 1607.01447)
[18] Fan W (for PHENIX Collaboration) Quark Matter 2019 - the XXVIIIth International Conference on Ultra-relativistic Nucleus-Nucleus Collisions (*Thermal photon production in Au+Au collisions*)
[19] Paquet J.-F 2017 *Private communication*
[20] Adare A *et al.* (PHENIX Collaboration) 2013 *Phys. Rev.* C **87** 054907 (*Preprint* 1208.1234)
[21] Novitzky N (PHENIX Collaboration) 2019 *PoS* **HardProbes2018** 185
[22] Aidala C *et al.* (PHENIX Collaboration) 2019 *Nature Phys.* **15** no. 3 214 (*Preprint* 1805.02973)
[23] Adare A *et al.* (PHENIX Collaboration) 2016 *Phys. Rev.* C **93** 024901 (*Preprint* 1509.06727)
[24] Aamodt K *et al.* (ALICE Collaboration) 2011 *Phys. Rev. Lett.* **106** 032301 (*Preprint* 1012.1657)
[25] Adam J *et al.* (ALICE Collaboration) 2016 *Phys. Lett.* B **754** 235 (*Preprint* 1509.07324)
[26] Angelis A S *et al.* (CCOR Collaboration) 1980 *Phys. Lett.* B **94** 106
[27] Angelis A S *et al.* (CMOR Collaboration) 1989 *Nucl. Phys.* B **327** 541; Akesson T *et al.* (AFS Collaboration) 1990 *Sov. J. Nucl. Phys.* **51** 836